ACSNANO
www.acsnano.org
ARTICLE

Ultrasensitive Vertical Piezotronic Transistor Based on ZnO Twin Nanoplatelet

Longfei Wang,[†] Shuhai Liu,[‡] Xiaolong Feng,[§] Qi Xu,[∥] Suo Bai,[∥] Laipan Zhu,[†] Libo Chen,[†] Yong Qin,[*,‡] and Zhong Lin Wang[*,†,⊥]

[†]Beijing Institute of Nanoenergy and Nanosystems, Chinese Academy of Sciences, National Center for Nanoscience and Technology (NCNST), Beijing 100083, China

[‡]School of Advanced Materials and Nanotechnology, Xidian University, Xi'an 710071, China

[§]Microsystems and Terahertz Research Center, China Academy of Engineering Physics, Chengdu, Sichuan 610200, China

[∥]Institute of Nanoscience and Nanotechnology, School of Physical Science and Technology, Lanzhou University, Gansu 730000, China

[⊥]School of Material Science and Engineering, Georgia Institute of Technology, Atlanta, Georgia 30332, United States

Supporting Information

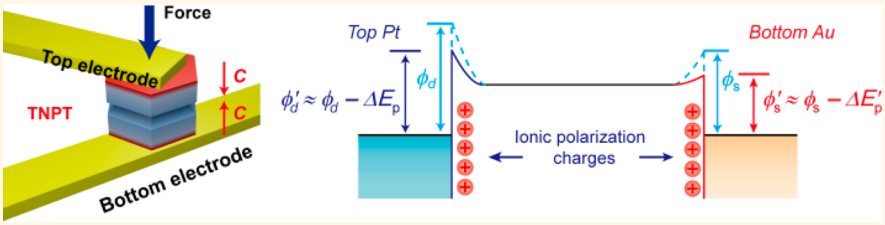

ABSTRACT: **High sensitivity of pressure/strain sensors is the key to accurately evaluating external mechanical stimuli and could become more important in future generations of human−machine interfaces and artificial skin. Here we report the study of a two-terminal piezotronic transistor based on ZnO twin nanoplatelets (TNPT). Owing to the mirror symmetrical structure of ZnO twin nanplatelet, compressive pressure-induced positive piezoelectric polarization charges created at both metal−semiconductor interfaces can simultaneously lower both Schottky barrier heights and thus significantly modulate the carrier transport. Our device exhibits the highest pressure sensitivity of 1448.08−1677.53 meV/MPa, which is more than ∼20 times larger than the highest value reported previously, and a fast response time of <5 ms. In addition, it can be used as a photodector with an ultrahigh external photoresponsivity of ∼1.45 × 10^4 AW^{-1}, which is ∼10^5 times larger in magnitude than that of commercial UV photodetectors. The coupling between the mirror symmetrical structure and strong piezotronic effect in ZnO twin nanoplatelets may enable the development of ultrasensitive pressure/strain sensors for various applications such as artificial skin, health monitoring, and adaptive biomedical probes.**

KEYWORDS: *piezotronic transistor, high sensitivity, piezotronic effect, piezo-phototronic effect, ZnO twin nanoplatelet*

Considerable interest has been devoted to implementing ultrafast, high-sensitivity, and low-power pressure/strain sensors for their applications in smart skin, healthcare, and defense technology.[1−6] As for nanoscale pressure/strain measurement, various multifunctional tactile sensors have been developed based on nanotubes, nanowires (NWs), and nanofilms by using the piezoresistive effect of nanomaterial to measure the spatial distribution of mechanical actuations.[7−15] Although this scheme of pressure/strain sensing presents attractive approaches to achieving an intelligent system that can mimic the function of human skin, the pressure/strain sensitivity of them (gauge factor ∼0.06−850)[10,11,16−18] is still relatively low due to a lack of direct and active interface between electronics and mechanical irritations.

Recently, strain-gated piezotronic transistors with two-terminal metal−semiconductor−metal structure were invented by using the piezoelectric semiconductor NWs with wurtzite structure (such as ZnO and GaN) or two-dimensional (2D) MoS_2 flakes.[19−23] The piezoelectric polarization charge-induced piezopotential in the NW or flake at the metal−semiconductor interfaces can directly control the transport characteristics of the piezotronic transistor through controlling the Schottky barrier heights (SBHs). The magnitude and polarity of the piezopotential within the piezoelectric semiconductor change according to the local stress.[6] The piezotronic transistor can directly convert the mechanical irritation into electrical signals without applying gate voltage, so that it has been already used

Received: February 26, 2017
Accepted: April 14, 2017
Published: April 14, 2017

DOI: 10.1021/acsnano.7b01374
ACS Nano XXXX, XXX, XXX−XXX

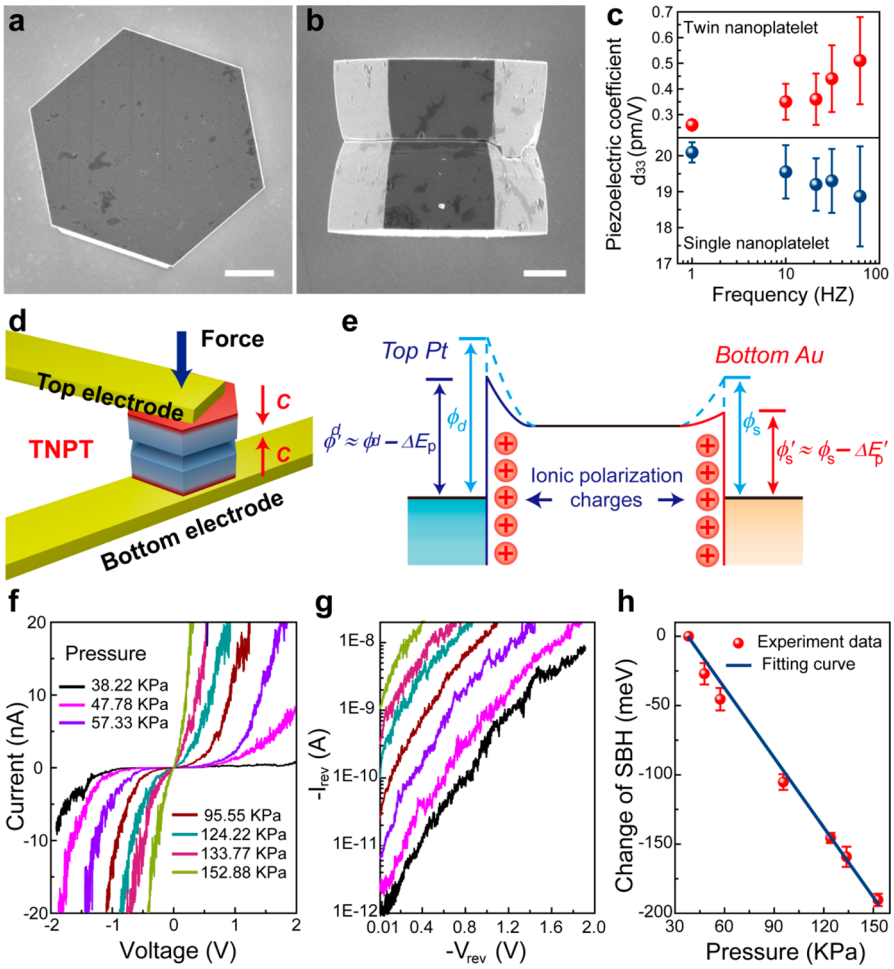

Figure 1. Top view (a) and side view (b) scanning electron micrographs of ZnO twin nanoplatelet. The scale bar indicates 1 μm. (c) Piezoelectric coefficient d_{33} of ZnO single and twin nanoplatelet acquired with different frequency. (d) Schematic illustration of TNPT. The red arrows represent the positive *c* axes of ZnO twin nanoplatelet. (e) Band diagrams of the working mechanism of TNPT. (f) The modulation of carrier transport by pressure in a TNPT, which shows the characteristic of piezotronic effect. (g) Current presented in semilog form *vs* voltage under reverse bias condition. (h) Calculated SBHs change as a linear function of the applied pressure shows that the modulation effect of applied pressure on the SBHs, demonstrating the extreme sensitivity of TNPT.

as active tactile sensors and self-emitting light strain sensors for tactile imaging.[6,19] These sensors have shown great potential applications in smart skin, human−machine interface, and bioimaging. However, due to the polar *c* axis orientation of NWs and armchair orientation of 2D flakes, the strain-induced piezopotentials at two contacts of a piezotronic transistor are opposite, which will result in converse modulation on local SBHs of the metal−semiconductor contacts and limit the pressure/strain sensitivity of the piezotronic transistor. Moreover, the buckling effect[24] among NWs and relative low piezoelectric coefficient of 2D flakes[21] also have negative influence on the pressure/strain sensitivity. To improve the pressure/strain sensitivity of the piezotronic transistor, it is important to develop devices whose SBHs of metal−semiconductor Schottky contacts can be modulated more effectively through strain.

Here we report a kind of two-terminal piezotronic transistor based on a ZnO twin nanoplatelet (TNPT) with the highest pressure sensitivity of 1448.08−1677.53 meV/MPa (gauge factor 2.9−9.4 × 10^9), which is ∼50 times larger than the reported NW-bundle-based piezotronic transistors.[6] Additionally, upon UV irradiation, we have also observed the TNPT's large external photoresponsivity of ∼1.45 × 10^4 AW^{-1}, which is about 100,000 times higher that of the commercial UV photodetectors.[25,26] This improvement can be understood as following: The compressive pressure-induced positive piezoelectric polarization charges at both ends of ZnO twin nanoplatelet can effectively lower the Schottky barriers height at both ZnO−metal contacts, which improves the charge carrier transport across the ZnO−metal interfaces and enhances the pressure/strain sensing.

RESULTS AND DISCUSSION

To develop an approach for an ultrasensitive piezotronic transistor, we synthesized a type of ZnO twin nanoplatelet. The scanning electron microscopy (SEM) images (Figures 1a,b and S1) show the ZnO twin nanoplatelet has a hexagonal shape, with a mirror symmetrical structure. Figure S2 shows the X-ray diffraction (XRD) pattern of twin nanoplatelets (red curve), which can be indexed to the wurtzite structure. As the most important factor of piezoelectric material, the effective piezoelectric coefficient d_{33} (Figures 1c and S3) of ZnO single nanoplatelet (blue curve) and twin nanoplatelet (red curve) were measured by piezoresponse force microscopy (PFM). They are found to be frequency dependent, which may be due to the imperfect electrical contact at the interface or surface

DOI: 10.1021/acsnano.7b01374
ACS Nano XXXX, XXX, XXX−XXX

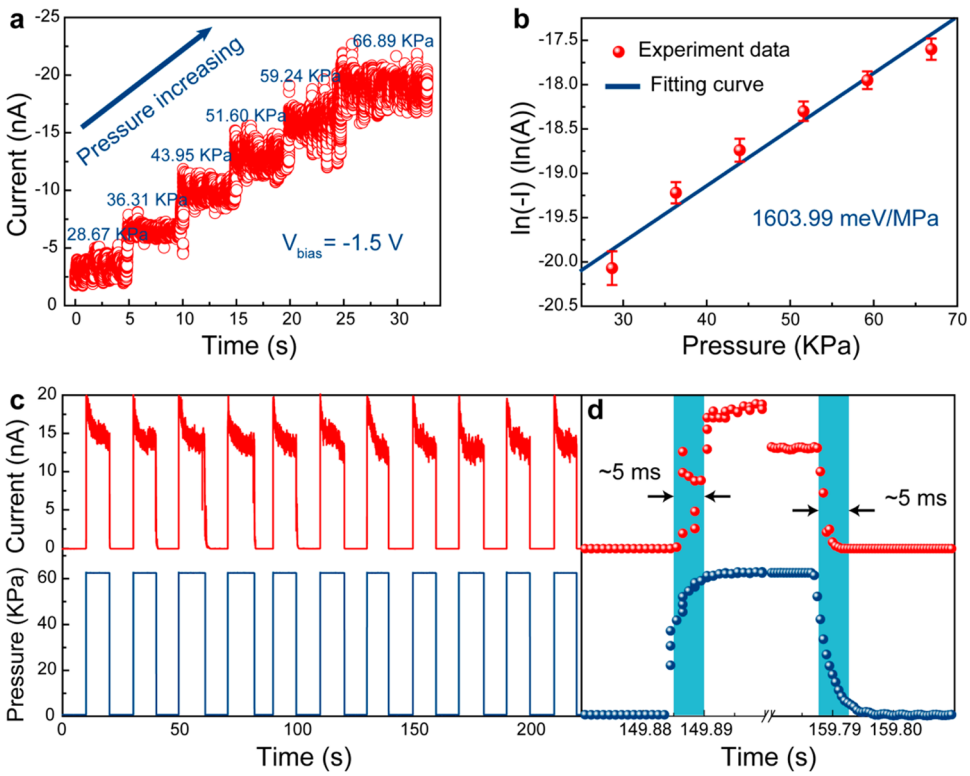

Figure 2. (a) The current of the TNPT increased step-by-step as the pressure increased. (b) ln(I)−P curve demonstrates a linear relationship between ln(I) and the applied pressure, showing the extreme sensitivity and indicating the modulation effect of applied pressure on conductance. (c) Current response to a pressure pulse, showing the repeatability of the pressure-switching response at 1.5 V bias. (d) Time response of the current between 145 and 165 s.

charge effect. The d_{33} of ZnO single nanoplatelet (Figure S1) is about 18.9−22.5 pm/V,[24] which is relatively high compared with the previous reported values (Table S1), whereas the measured d_{33} value of ZnO twin nanoplatelet is negligible because of the mirror symmetrical structure. With the mirror symmetrical geometry and strong piezoelectricity presented in a single nanoplatelet (half part of twin nanoplatelet), the ZnO twin nanoplatelet is a suitable candidate to serve as the piezoelectric component of piezotronic nanodevices.

Based on the well-aligned ZnO twin nanoplatelets, a kind of two-terminal TNPT is designed (Figures 1d and S4). The basic structure of the TNPT consists of one ZnO twin nanoplatelet, bottom Au and top Pt electrodes. ZnO twin nanoplatelet has an axial strain when subjected to the normal compressive force, as shown in Figure 1d. Owing to the mirror symmetrical structure of ZnO twin nanoplatelet, piezopotentials distribute along the ZnO twin nanoplatelet with positive piezoelectric polarization charges presenting at the top and bottom surfaces of ZnO twin nanoplatelet, distributing within a thickness of 1−2 atomic layers.[27,28] They can simultaneously lower both Schottky barriers of the ZnO−metal contacts and hence significantly increase the transport conductance of TNPT. Therefore, the carrier transport characteristic across the Schottky barrier is controlled effectively by the strain-induced positive piezopotential (Figure 1e). Based on this fundamental principle, a vertical piezotronic transistor based on a ZnO twin nanoplatelet is introduced to gigantically modify the electronic transport property of piezotronic nanodevices by designing the dual Schottky junctions' synergistic modulation utilizing ZnO twin nanoplatelet.

Next, the electrical transport properties of TNPTs under various pressures were characterized. Figure 1f shows the pressure-dependent I_{ds}−V_{ds} characteristics of TNPT. The current dramatically increases as the pressure increased and gradually changes from the Schottky characteristic curve to the ohmic characteristic curve, which indicates that the SBHs gradually decreased with increased pressure. To better understand the regulation mechanism and calculate the change of SBHs under various pressures, we used the classic Schottky theory to derive the change of SBHs from the I_{ds}−V_{ds} curves. Since all experiments were taken at room temperature and the doping concentrations of the ZnO twin nanoplatelet is high, it is most suitable for us to use the thermionic-field-emission (TFE) and thermionic-emission-diffusion (TED) models to analyze the experimental results. In the TFE and TED models, ln(I) is approximately proportional to V and $V^{1/4}$. We found that the ln(I) − V is almost linear, which indicates that the dominant process in our experiment was TFE (Figures 1g and S6−7). According to the classic Schottky theory,[22,29] the changes of SBH ($\Delta\varphi$) can be estimated by the following formula: $\Delta\varphi = -kT\ln(I_{strain}/I_{free})$. Based on this formula, the average $\Delta\varphi$ as a function of pressure is obtained (Figures 1h and S7), which is approximately linear and consistent with the piezotronic model. The result shows that SBHs decrease as the compressive strain increased, which demonstrates that the compressive pressure-induced positive piezoelectric polarization charges that exist at both metal−ZnO interfaces can significantly lower the Schottky barrier. This deduction is further confirmed by the transport characteristics of TNPT devices with single Schottky junction (Figures S5 and 8−11). Through the detailed analysis, we can conclude the piezotronic

DOI: 10.1021/acsnano.7b01374
ACS Nano XXXX, XXX, XXX−XXX

effect is the dominant mechanism of the carrier transport property of TNPT.

The pressure sensitivity of TNPT is shown in Figure 2a. We applied an increasing pressure on the TNPT and measured the current response. The TNPT demonstrated an extreme sensitivity in low-pressure regions (from several kPa to hundreds of kPa), which has huge potential in tactile sensing such as human−electronics interfacing and smart skin. A plot of ln(I) curve *vs* applied pressures (Figure 2b) shows that the current increases exponentially with applied pressure, which is consistent with the above analysis and indicates the modulation effect of applied pressure on TNPT's conductance. The pressure sensitivity (defined as $S = d_{SBH}/d_{pressure}$, Figure S12) of TNPT calculated here is about 1448.08−1677.53 meV/MPa, which is the highest one among all previous reports (Table 1).

Table 1. Comparison of Pressure Sensitivity from Piezotronic Transistors Based on Different Piezoelectric Semiconductor Materials with Various Geometrical Parameters

materials and morphology[a]		pressure sensitivity (meV/MPa)	force method	ref
CdSe	NW	∼0.677	normal force	30
ZnO	NW	0.083−0.422	normal force	29
GaN	NW	0.212−0.24	normal force	31
ZnO	NW Cluster	0.287−0.318	normal force	32
ZnO	NW cluster	<33.39	normal force	6
ZnO	nanoplatelet	60.97−78.23	normal force	24
ZnO	twin nanoplatelet	1448.08−1677.53	normal force	this work

[a]NW: Nanowire as the single piezoelectric component. NW cluster: Nanowire cluster as the single piezoelectric component. Nanoplatelet: Nanoplatelet as the single piezoelectric component.

It far exceeds that of other NW-based piezotronic transistors[29−32] and is more than 20 times higher than the highest one of previous reports.[24] Furthermore, as a strain sensor, the performance of TNPT is also characterized by a gauge factor, which is defined as the normalized current variation divided by strain, generally written as $[\Delta I(\varepsilon)/I(0)]/\Delta\varepsilon$. The gauge factor of our device demonstrated here is $2.9-9.4 \times 10^9$, which is the highest one by now compared to the previously reported values (Table S2). The key factor in achieving the extreme pressure sensitivity is the dual Schottky barriers' synergistic modulation of TNPT.

In order to illustrate the responsiveness of 2DPT to the external stimuli, the current response to periodic force pulses of TNPT was measured under constant biases (Figure 2c), which shows that the modulation of strain-induced positive piezopotential on the current is reversible. The current increases from ∼0.043 nA to ∼19.6 nA after applying a ∼62.5 KPa normal pressure on TNPT, which can be considered as the "off" and "on" states. The on−off ratio is about 455, which can be further increased by enlarging the pressure. Furthermore, no obvious degradation in TNPT operation could be observed after a reliability test, suggesting the good reliability in the device operation. The response time was monitored by using the AFM measurement system. The current responds quickly to a change of pressure of <5 ms (Figure 2d), which is far less than the response time of human fingertips (∼30−50 ms), and it makes TNPTs have great potential in the applications of tactile sensors with ultrafast response.

To better explain the experimental results of ultrahigh pressure/strain sensitivity of TNPT and estimate the modulate effect of the strain-induced piezopotential on SBH of ZnO−metal contacts, we developed a 3D finite element (FE) model with COMSOL Multiphysics, as schematically shown in Figures 3 and S13. The previously reported piezotronic transistors usually consist of metal electrodes and a NW or 2D flake (such as ZnO, GaN, and MoS_2). In this simulation setup, under normal compressive pressure, the piezoelectric charges are accumulated at both Schottky contacts (Figure 3a). Because the orientation of the polar c axis in the as-synthesized NWs, the positive piezopotential is induced at the bottom Schottky contact, which lowers the SBH and thus increases the transport conductance of the piezotronic transistor, while a negative piezopotential is induced at the top Schottky contact, which rises the SBH and thus decreases the transport property of the piezotronic transistor (Figure 3b inset). The strain-induced piezopotentials at both Schottky contacts of the piezotronic transistor are opposite, resulting in a converse modulation on local SBHs of the metal−semiconductor Schottky contacts, thus limiting the pressure/strain sensitivity of the piezotronic transistor. It is further demonstrated by the theoretical calculated current−voltage curves of the NW-based piezotronic transistor at different applied strains (Figure 3b), where the converse modulation trend of electric transport was observed under opposite drain biases.

The theoretical simulation of a strained TNPT used in this work was investigated, as shown in Figure 3c,d. Owing to the mirror symmetrical structure of a ZnO twin nanoplatelet, piezopotentials distribute along the ZnO twin nanoplatelet with positive piezoelectric polarization charges presenting at the top and bottom surfaces (Figure 3c), which can both lower the SBHs and hence significantly enhance the transport conductance of a TNPT (Figure 3d inset). The theoretical calculated current−voltage curves of a TNPT with different strains are shown in Figure 3d. By increasing the compressive strain, the transport conductance of the TNPT was synchronously increased in both forward bias and reverse bias, which is in accordance with the experimental data. Our simulation demonstrates the dual Schottky junction synergistic modulation of TNPT, which results in high pressure/strain sensitivity.

Next, the photosensing property of TNPT is explored by applying a 365 nm wavelength UV light stimuli. By changing the intensity of the UV light, a series of $I_{ds}-V_{ds}$ characteristics were measured (Figure S14). The results show a good photoresponse (Supporting Information, Note 6). Then the UV detection performance of TNPT is enhanced by piezo-phototronic effects. As shown in Figure 4a, the $I_{ds}-V_{ds}$ characteristics of TNPT under constant illumination intensity and various pressures are nonlinear at small bias voltages. The current increases by several orders of magnitude when the compressive pressure increased from 24.84 KPa to 152.88 KPa, indicating that the change of SBHs are the dominant factor for the transport characteristic.

To deeply explore the mechanism of current increase, we explore the photosensitivity of our photodetector, defined as $\Delta I = (I_{light} - I_{dark})/I_{dark}$, where I_{light} and I_{dark} (Figure S15) are the

DOI: 10.1021/acsnano.7b01374
ACS Nano XXXX, XXX, XXX−XXX

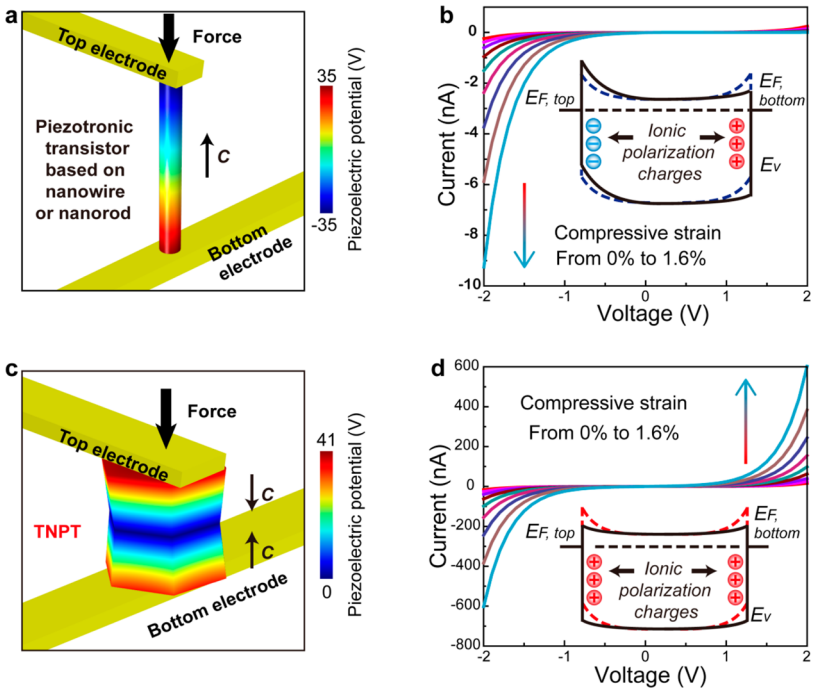

Figure 3. (a) Schematic of a piezotronic transistor based on a traditional NW or nanorod under a compressive strain of 0.001 simulated by a FE analysis method. (b) Theoretical calculation the current−voltage curves for the NW-based piezotronic transistor at different applied strains. Inset: Schematic band diagram of a NW-based piezotronic transistor before (blue line) and after (black line) applying a compressive force. (c) Schematic of a TNPT under compressive strain of 0.001 simulated by a FE analysis method. (d) Theoretical calculation the current−voltage curves for the TNPT at different applied strains. Inset: Schematic band diagram of a ZnO twin nanoplatelet-based piezotronic transistor before (red line) and after (black line) applying a compressive force.

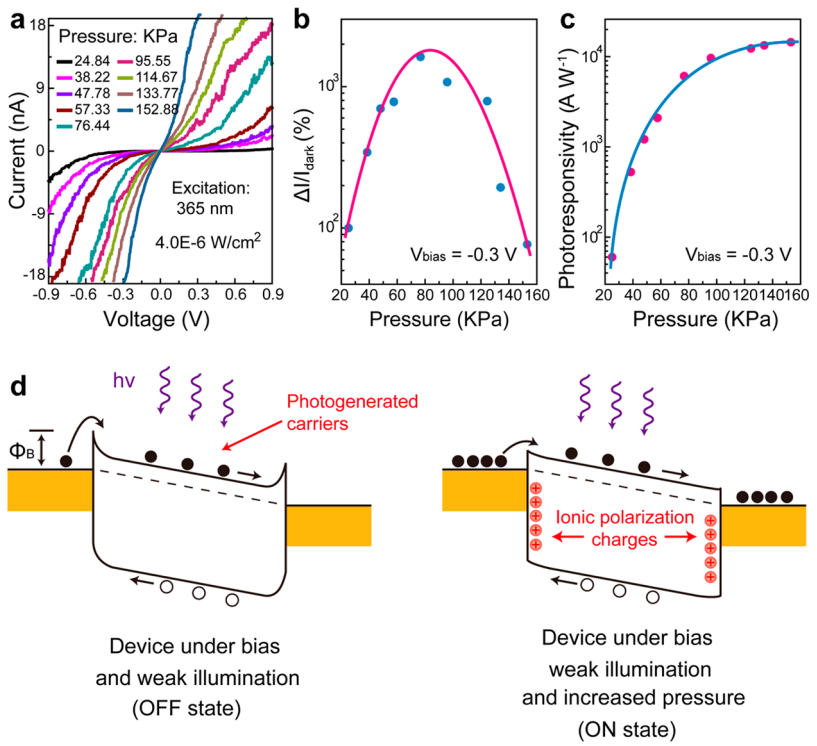

Figure 4. Photoresponse of TNPT under various pressures. (a) Drain−source characteristic of the TNPT with constant illumination and under different pressures. Photosensitivity (b) and photoresponsivity (c) of the TNPT as a function of pressures, showing high sensitivity. (d) Band diagram of the TNPT under UV irridiation illustrates the working mechanism of enhancement mode TNPT. Φ_B represents the SBH.

drain current with and without illumination under a specific compressive pressure, respectively. The photosensitivity of the TNPT under various strains was derived (Figure 4b), which shows that the maximum value is ∼1625% by applying a

DOI: 10.1021/acsnano.7b01374
ACS Nano XXXX, XXX, XXX−XXX

pressure of 76.44 kPa on the TNPT. When further increasing the pressure, the photosensitivity begins to decrease, which may be due to the competing mechanism between the screening effect by the photogenerated free charge carriers and piezoelectric polarization charges. Under the small pressure, the free carriers induced by weak light can partially shield the piezoelectric polarization charges existing at the ZnO−metal interfaces. While under the large pressure, the modulation effect of strain-induced piezoelectric polarization charges on SBHs begins to dominate the carrier transport across the Schottky contacts.

Another important quality factor of the photodetector is an external photoresponsivity R defined as $R = (I_{light} - I_{dark})/P_{illumination}$, where $P_{illumination}$ is the illumination power on the TNPT. It can be seen that there is a monotonous increase of R without saturation and the largest R value reaching 1.45×10^4 AW^{-1} when applying a pressure of 152.88 kPa on the TNPT (Figure 4c). This R value is $\sim 10^5$ times larger than that of commercial UV photodetectors (0.1−0.2 AW^{-1}),[25,26] $\sim 10^6$ times larger than that of a Si/ZnO core−shell NW array photodetector (1.0×10^{-2} AW^{-1}, 480 nm, −1 V),[33] and $\sim 10^4$ times larger than that of a Si/CdS core−shell NW network photodetector (<1 AW^{-1}, 480 nm, −1 V).[34] These demonstrate that TNPTs have great potential applications in photodetectors with high photosensitivity.

The enhanced performance of our photodetector by piezo-phototronic effect can be explained by energy band diagrams (Figure 4d). In the OFF state, the photogenerated electron−hole pairs can be separated by applying an external bias. However, large Schottky barriers are formed at both sides of the ZnO−metal contacts, which would result in little photocurrent flowing under weak illumination and low bias. In the ON state, upon applying the normal stress, because of the mirror symmetrical structure of ZnO twin nanoplatelet, positive piezoelectric charges are accumulated at both Schottky contacts, which can lower both Schottky barrier's heights and significantly improve the charge separation. In addition to the increase of photocurrent, the local dark current also contributes to the device currents.

CONCLUSIONS

To summarize, a kind of TNPT with the highest pressure/strain sensitivity to date has been developed. Owing to the mirror symmetrical structure of a ZnO twin nanoplatelet with strong piezotronic effect, the compressive pressure-induced positive piezoelectric polarization charges at both metal−semiconductor interfaces can effectively lower the SBH at both ZnO−metal contacts and improve the charge carrier transport across the ZnO−metal interfaces. The TNPT exhibits a high-pressure sensitivity of 1448.08−1677.53 meV/MPa (gauge factor 2.9−9.4 $\times 10^9$) and a fast response time of <5 ms. Moreover, it shows the characteristics of a piezo-phototronic photodetector with tunable photosensitivity and photoresponsivity (1.45×10^4 AW^{-1}). Since the TNPT can directly convert the mechanical force into electrical signals without applying gate voltage, it has a great competitive advantage as the fundamental component for piezotronics and piezo-phototronics. This work shows great potential for designing the next generation of two terminal vertical transistors with ultrahigh sensitivity, which have great applications in many fields such as adaptive artificial skin, biomedical probes, and health monitoring.

METHODS

Synthesis of ZnO Twin Nanoplatelets. In the synthesis process, 30 mL of aqueous solution containing 91 mM $Zn(CH_3COO)_2$ and 151 mM tris(hydroxymethyl)methyl aminomethane (THAM) was prepared in a glass container. Then, the glass was placed in an oven at 95 °C. ZnO twin nanoplatelets appeared in 2 h and were collected for characterization and device fabrication.

Material Characterizations. The morphology and structure of ZnO twin nanoplatelets were characterized using a scanning electron microscope (Hitachi SU8020), PANalytical X'Pert PRO diffractometer (Almelo, The Netherlands) with Cu KR radiation (λ = 0.15418 nm). The effective piezoelectric coefficient d_{33} was measured by PFM (MFP-3D from Asylum Research).

Fabrication Process of ZnO Twin Nanoplatelet-Based Piezotronic Transistors. A SiO_2/Si substrate was cleaned and dried first. Then the substrate was deposited with Cr/Au (5 nm/60 nm) by RF magnetron sputtering. A proper amount of ZnO twin nanoplatelets were dispersed into ethanol under ultrasonication for several minutes at room temperature to obtain a homogeneous ethanol dispersion. The ZnO twin nanoplatelet ethanol dispersion was dropped on the prepared substrate, and then the substrates were blown dry by compressed N_2 quickly. This procedure was repeated for several times.

Optical and Electrical Measurements of Piezotronic (Photo)-transistor. $I-V$ characteristics of the device were measured by using a conductive AFM system (MFP-3D Asylum Research) with a Pt-coated Si AFM probe, which has a spring constant of 34.27 nN/nm and an inverse optical lever sensitivity (InvOLS) of 90.55 nm/V. The optical input stimuli were provided by a common Hg−Xe lamp (LC8-TLSX1046C03). A 365 nm UV light source was used to achieve the various illumination intensities.

ASSOCIATED CONTENT

Supporting Information

The Supporting Information is available free of charge on the ACS Publications website at DOI: 10.1021/acsnano.7b01374.

Additional information and figures, including experimental details, materials, methods, and supplementary notes (PDF)

AUTHOR INFORMATION

Corresponding Authors

*E-mail: zhong.wang@mse.gatech.edu

*E-mail: qinyong@lzu.edu.cn.

ORCID

Zhong Lin Wang: 0000-0002-5530-0380

Notes

The authors declare no competing financial interest.

ACKNOWLEDGMENTS

This research was supported by the "thousands talents" program for pioneer researcher and his innovation team, China, National Natural Science Foundation of China (grant nos. 51322203, 51472111, 51432005, 5151101243, and 51561145021), the National Key R&D Project from Minister of Science and Technology (2016YFA0202704), and the National Program for Support of Top-Notch Young Professionals.

REFERENCES

(1) Ko, H. C.; Stoykovich, M. P.; Song, J. Z.; Malyarchuk, V.; Choi, W. M.; Yu, C. J.; Geddes, J. B.; Xiao, J. L.; Wang, S. D.; Huang, Y. G.; Rogers, J. A. A Hemispherical Electronic Eye Camera based on Compressible Silicon Optoelectronics. *Nature* **2008**, *454*, 748−753.

(2) Tian, B. Z.; Liu, J.; Dvir, T.; Jin, L. H.; Tsui, J. H.; Qing, Q.; Suo, Z. G.; Langer, R.; Kohane, D. S.; Lieber, C. M. Macroporous Nanowire Nanoelectronic Scaffolds for Synthetic Tissues. *Nat. Mater.* **2012**, *11*, 986−994.
(3) Wang, C.; Hwang, D.; Yu, Z. B.; Takei, K.; Park, J.; Chen, T.; Ma, B. W.; Javey, A. User-Interactive Electronic Skin for Instantaneous Pressure Visualization. *Nat. Mater.* **2013**, *12*, 899−904.
(4) Keplinger, C.; Sun, J. Y.; Foo, C. C.; Rothemund, P.; Whitesides, G. M.; Suo, Z. G. Stretchable, Transparent, Ionic Conductors. *Science* **2013**, *341*, 984−987.
(5) Dvir, T.; Timko, B. P.; Brigham, M. D.; Naik, S. R.; Karajanagi, S. S.; Levy, O.; Jin, H. W.; Parker, K. K.; Langer, R.; Kohane, D. S. Nanowired Three-Dimensional Cardiac Patches. *Nat. Nanotechnol.* **2011**, *6*, 720−725.
(6) Wu, W. Z.; Wen, X. N.; Wang, Z. L. Taxel-Addressable Matrix of Vertical-Nanowire Piezotronic Transistors for Active and Adaptive Tactile Imaging. *Science* **2013**, *340*, 952−957.
(7) He, R.; Yang, P. Giant Piezoresistance Effect in Silicon Nanowires. *Nat. Nanotechnol.* **2006**, *1*, 42−46.
(8) Tombler, T. W.; Zhou, C. W.; Alexseyev, L.; Kong, J.; Dai, H. J.; Lei, L.; Jayanthi, C. S.; Tang, M. J.; Wu, S. Y. Reversible Electromechanical Characteristics of Carbon Nanotubes under Local-Probe Manipulation. *Nature* **2000**, *405*, 769−772.
(9) Stampfer, C.; Helbling, T.; Obergfell, D.; Schoberle, B.; Tripp, M. K.; Jungen, A.; Roth, S.; Bright, V. M.; Hierold, C. Fabrication of Single-Walled Carbon-Nanotube-based Pressure Sensors. *Nano Lett.* **2006**, *6*, 233−237.
(10) Takei, K.; Takahashi, T.; Ho, J. C.; Ko, H.; Gillies, A. G.; Leu, P. W.; Fearing, R. S.; Javey, A. Nanowire Cctive-Matrix Circuitry for Low-Voltage Macroscale Artificial Skin. *Nat. Mater.* **2010**, *9*, 821−826.
(11) Mannsfeld, S. C. B.; Tee, B. C. K.; Stoltenberg, R. M.; Chen, C. V. H.-H.; Barman, S.; Muir, B. V. O.; Sokolov, A. N.; Reese, C.; Bao, Z. N. Highly Sensitive Flexible Pressure Sensors with Microstructured Rubber Dielectric Layers. *Nat. Mater.* **2010**, *9*, 859−864.
(12) Lipomi, D. J.; Vosgueritchian, M.; Tee, B. C. K.; Hellstrom, S. L.; Lee, J. A.; Fox, C. H.; Bao, Z. N. Skin-Like Pressure and Strain Sensors based on Transparent Elastic Films of Carbon Nanotubes. *Nat. Nanotechnol.* **2011**, *6*, 788−792.
(13) Zhang, Z.; Fan, R.; Shi, Z.; Pan, S.; Yan, K.; Sun, K.; Zhang, J.; Liu, X.; Wang, X.; Dou, S. Tunable Negative Permittivity Behavior and Conductor-Insulator Transition in Dual Composites Prepared by Selective Reduction Reaction. *J. Mater. Chem. C* **2013**, *1*, 79−85.
(14) Sekitani, T.; Yokota, T.; Zschieschang, U.; Klauk, H.; Bauer, S.; Takeuchi, K.; Takamiya, M.; Sakurai, T.; Someya, T. Organic Nonvolatile Memory Transistors for Flexible Sensor Arrays. *Science* **2009**, *326*, 1516−1519.
(15) Ahn, J. H.; Kim, H. S.; Lee, K. J.; Jeon, S.; Kang, S. J.; Sun, Y. G.; Nuzzo, R. G.; Rogers, J. A. Heterogeneous Three-Dimensional Electronics by Use of Printed Semiconductor Nanomaterials. *Science* **2006**, *314*, 1754−1757.
(16) Cao, J.; Wang, Q.; Dai, H. J. Electromechanical Properties of Metallic, Quasimetallic, and Semiconducting Carbon Nanotubes under Stretching. *Phys. Rev. Lett.* **2003**, *90*, 157601.
(17) Yamada, T.; Hayamizu, Y.; Yamamoto, Y.; Yomogida, Y.; Izadi-Najafabadi, A.; Futaba, D. N.; Hata, K. A. Stretchable Carbon Nanotube Strain Sensor for Human-Motion Detection. *Nat. Nanotechnol.* **2011**, *6*, 296−301.
(18) Pang, C.; Lee, G. Y.; Kim, T. I.; Kim, S. M.; Kim, H. N.; Ahn, S. H.; Suh, K. Y. A Flexible and Highly Sensitive Strain-Gauge Sensor Using Reversible Interlocking of Nanofibres. *Nat. Mater.* **2012**, *11*, 795−801.
(19) Pan, C. F.; Dong, L.; Zhu, G.; Niu, S. M.; Yu, R. M.; Yang, Q.; Liu, Y.; Wang, Z. L. High-Resolution Electroluminescent Imaging of Pressure Distribution Using a Piezoelectric Nanowire LED Array. *Nat. Photonics* **2013**, *7*, 752−758.
(20) Zhu, L.; Wang, L.; Xue, F.; Chen, L.; Fu, J.; Feng, X.; Li, T.; Wang, Z. L. Piezo-Phototronic Effect Enhanced Flexible Solar Cells based on n-ZnO/p-SnS Core-Shell Nanowire Array. *Adv. Sci.* **2017**, *4*, 1600185.
(21) Wu, W.; Wang, L.; Li, Y.; Zhang, F.; Lin, L.; Niu, S.; Chenet, D.; Zhang, X.; Hao, Y.; Heinz, T. F.; Hone, J.; Wang, Z. L. Piezoelectricity of Single-Atomic-Layer MoS_2 for Energy Conversion and Piezotronics. *Nature* **2014**, *514*, 470−474.
(22) Zhou, Y. S.; Hinchet, R.; Yang, Y.; Ardila, G.; Songmuang, R.; Zhang, F.; Zhang, Y.; Han, W. H.; Pradel, K.; Montes, L.; Mouis, M.; Wang, Z. L. Nano-Newton Transverse Force Sensor Using a Vertical GaN Nanowire based on the Piezotronic Effect. *Adv. Mater.* **2013**, *25*, 883−888.
(23) Wang, L.; Liu, S.; Wang, Z.; Zhou, Y.; Qin, Y.; Wang, Z. L. Piezotronic Effect Enhanced Photocatalysis in Strained Anisotropic ZnO/TiO_2 Nanoplatelets *via* Thermal Stress. *ACS Nano* **2016**, *10*, 2636−2643.
(24) Liu, S.; Wang, L.; Feng, X.; Wang, Z.; Xu, Q.; Bai, S.; Qin, Y.; Wang, Z. L. Ultrasensitive 2D ZnO Piezotronic Transistor Array for High Resolution Tactile Imaging. *Adv. Mater.* **2017**, 1606346.
(25) Monroy, E.; Omnes, F.; Calle, F. Wide-Bandgap Semiconductor Ultraviolet Photodetectors. *Semicond. Sci. Technol.* **2003**, *18*, R33−R51.
(26) Zou, J.; Zhang, Q.; Huang, K.; Marzari, N. Ultraviolet Photodetectors based on Anodic TiO_2 Nanotube Arrays. *J. Phys. Chem. C* **2010**, *114*, 10725−10729.
(27) Wang, Z. L. Progress in Piezotronics and Piezo-Phototronics. *Adv. Mater.* **2012**, *24*, 4632−4646.
(28) Zhang, Y.; Liu, Y.; Wang, Z. L. Fundamental Theory of Piezotronics. *Adv. Mater.* **2011**, *23*, 3004−3013.
(29) Han, W. H.; Zhou, Y. S.; Zhang, Y.; Chen, C. Y.; Lin, L.; Wang, X.; Wang, S. H.; Wang, Z. L. Strain-Gated Piezotronic Transistors based on Vertical Zinc Oxide Nanowires. *ACS Nano* **2012**, *6*, 3760−3766.
(30) Zhou, Y. S.; Wang, K.; Han, W. H.; Rai, S. C.; Zhang, Y.; Ding, Y.; Pan, C. F.; Zhang, F.; Zhou, W. L.; Wang, Z. L. Vertically Aligned CdSe Nanowire Arrays for Energy Harvesting and Piezotronic Devices. *ACS Nano* **2012**, *6*, 6478−6482.
(31) Zhao, Z. F.; Pu, X.; Han, C. B.; Du, C. H.; Li, L. X.; Jiang, C. Y.; Hu, W. G.; Wang, Z. L. Piezotronic Effect in Polarity-Controlled GaN Nanowires. *ACS Nano* **2015**, *9*, 8578−8583.
(32) Han, X.; Du, W. M.; Yu, R. M.; Pan, C. F.; Wang, Z. L. Piezo-Phototronic Enhanced UV Sensing based on a Nanowire Photodetector Array. *Adv. Mater.* **2015**, *27*, 7963−7969.
(33) Sun, K.; Jing, Y.; Park, N.; Li, C.; Bando, Y.; Wang, D. Solution Synthesis of Large-Scale, High-Sensitivity ZnO/Si Hierarchical Nanoheterostructure Photodetectors. *J. Am. Chem. Soc.* **2010**, *132*, 15465−15467.
(34) Manna, S.; Das, S.; Mondal, S. P.; Singha, R.; Ray, S. K. High Efficiency Si/CdS Radial Nanowire Heterojunction Photodetectors Using Etched Si Nanowire Templates. *J. Phys. Chem. C* **2012**, *116*, 7126−7133.

DOI: 10.1021/acsnano.7b01374
ACS Nano XXXX, XXX, XXX−XXX